

ISSN 1840-4855

e-ISSN 2233-0046

Original scientific article

<http://dx.doi.org/10.70102/afts.2026.1835.264>

## SYNTHESIS AND CHARACTERISTICS OF ZNO THIN FILMS DEPOSITED VIA THE SILAR METHOD: IMPACT OF THE NUMBER OF CYCLES

Anwar Qasim Ahmed<sup>1\*</sup>, Inass Abdulah Zgair<sup>2</sup>, Adel H. Omran Alkhayatt<sup>3</sup>

<sup>1\*</sup>Assistant Professor, Faculty of Science, University of Kufa, Najaf, Iraq.

e-mail: [anwarq.hameed@uokufa.edu.iq](mailto:anwarq.hameed@uokufa.edu.iq), orcid: <https://orcid.org/0000-0002-8112-5694>

<sup>2</sup>Assistant Professor, Faculty of Science, University of Kufa, Najaf, Iraq.

e-mail: [enasa.taha@uokufa.edu.iq](mailto:enasa.taha@uokufa.edu.iq), orcid: <https://orcid.org/0000-0001-9672-0640>

<sup>3</sup>Professor, College of Medicine, University of Alkafeel, Najaf, Iraq.

e-mail: [adelh.alkhayatt@alkafeel.edu.iq](mailto:adelh.alkhayatt@alkafeel.edu.iq), orcid: <https://orcid.org/0000-0001-8979-4502>

**Received: January 05, 2026; Revised: February 19, 2026; Accepted: April 09, 2026; Published: May 29, 2026**

### SUMMARY

The successive Ionic Layer Adsorption and Reaction (SILAR) process was used to form Zinc Oxide (ZnO) thin films on glass substrates, and deposition cycles of 5, 15, 20, and 25 were used to investigate the effect of the number of cycles on the structural and optical characteristics of the film. The X-ray diffraction (XRD) was determined to be a polycrystalline structure of ZnO, having the hexagonal wurtzite structure with a preferential orientation of the (100) plane. The size of the grain and crystallinity increased with the number of deposition cycles, and the density of dislocations reduced, which implies better quality of the film. The UV-Vis spectroscopy was used to determine the optical properties of the material, such as the optical band gap and absorbance. The findings indicated that the optical band gap was different in the range of 3.67 eV to 3.81 eV, with the largest band gap found in the 20-cycle sample. The absorbance reduced with an increase in the cycle number, indicating improved scattering and grain boundary effects with increasing number of cycles. The movies proved to be more transparent as the cycles were increased, and thus can be applied in the field of optoelectronics, where solar cells and light-emitting devices can be used. SILAR has emerged as an economical approach to prepare ZnO thin films and has provided an easy and effective methodology to regulate the film thickness and quality. The research also gives important information on the depositional cycle as it affects the characteristics of ZnO films, which is important in the optimization of ZnO thin films for different technological uses. Further research to improve the performance of the film, such as the refinement of the deposition parameters and the possibility of incorporating the films into the real world, such as solar cells, sensors, and transparent conductive layers, will be undertaken in the future.

**Key words:** *ZnO thin films, silar method, optical properties, grain size, optical band gap, deposition cycles, structural characterization.*

## INTRODUCTION

Zinc oxide (ZnO) composites in the nanoscale range reflect remarkable properties that vary as the preparation conditions change, so they are considered as potential candidates in the nanotechnology industry. The most important aspect of nanostructure represents a considerable surface-to-volume ratio; this characteristic gives the preference of nanostructure materials over bulk counterparts. Therefore, preferred electrical and optical properties are achieved with nanomaterials for physical and chemical applications such as light sensors, light-emitting diodes, solar cells, etc. [1]. These materials exhibit n-type semiconductor behavior with a direct band gap energy of 3.370 eV [2]. ZnO nanostructure as a thin film was prepared using the successive ionic layer adsorption and reaction (SILAR) method, which is regarded as a straightforward method since it involves minimal expenses and low-cost reagents compared with the other methods that involve complicated instruments such as applying high pressure and temperature arrangements. The SILAR method was first reported to prepare thin films of ZnO, and the results were later confirmed using a specialized technique referred to as an automated electro-pneumatic deposition setup [3][4].

The SILAR technique is based on putting two solutions, one anionic and one cationic, in two separate containers, which are considered a bath. A substrate of glass is repetitively (periodically) immersed in both cationic and anionic solutions, which leads to facilitating a heterogeneous reaction followed by film formation by agglomeration on the substrate surface, without any precipitation happening in the solution bath [5]. The deposition rate and thickness for the formed thin film were controlled by varying the deposition cycle time.

Zinc oxide was fabricated in the form of a thin film by utilising the thermal evaporation method, and it was found that transmittance values were observed in the NIR region, and the gap (3.4 eV). While XRD consequences indicated that the formed films were crystalline with a hexagonal wurtzite structure [6]. Moreover, fabrication of ZnO thin film via SILAR method is achieved for 15 dip cycles, then annealed at 450 °C for one hour, and they obtained optical band gap with (3.750) eV [7]. The prepared ZnO thin film on the substrate of glass and the Si (100) substrate via the RF sputtering technique exhibited a preferred orientation along the c-axis (002) with a phase of wurtzite structure associated with tensile strain [19]. They study optical transmittance values of 70–88% within the visible range for all the formed films [9][20].

This study investigates the effect of varying the number of cycles on the formed ZnO thin films that were deposited onto a glass substrate, which was submerged in solution to analyze and investigate the structural and optical properties.

Zinc Oxide (ZnO) thin films are a type of film that has exceptional optical and electrical characteristics, which have been utilized in the development of techniques like solar cells, light-emitting diodes, and sensor instruments. Of importance in this study is the low-cost Successive Ionic Layer Adsorption and Reaction (SILAR) approach through which the highly economical and efficient manner of creating ZnO thin films with control of their thickness and improved properties is achieved. This is especially significant when nanotechnology is considered, where nanoscale materials have a better surface-to-volume ratio, thus resulting in a higher physical and chemical property compared to bulk materials. The use of ZnO thin films in the area of optoelectronics, such as solar energy collection and transparent conductive layers in devices, renders the goal to maximize the structural and optical properties of films. This study would serve as an essential background on how to enhance the design and manufacture of high-performance ZnO thin films by exploring the impact of different deposition cycles to meet the future innovation of cost-effective and sustainable technology solutions.

1. The given study offers thorough research of the impact of the deposition cycles on the structural and optical characteristics of the ZnO thin films, providing considerable information concerning the impact of changes in the cycles on the grain size, crystallinity, and optical band gap.
2. The study indicates the efficiency of the SILAR approach in the creation of high-grade ZnO thin films at minimal expenditure, which has the opportunity to generate ZnO films on a large scale in optoelectronic applications, including solar cells and light-emitting devices.

3. This is significant in that through the correlation of the deposition cycles and optical characteristics of the films, i.e., transmittance and absorption, the study will provide valuable data in optimizing the work of ZnO thin films in practical devices, providing a way to enable better energy efficiency and functionality of future technological uses.

The outline of the paper is as follows: Section 1 contains the background and importance of ZnO thin films and the SILAR process of their deposition. Section 2 presents a literature review that is detailed and covers the recent developments in the deposition methods of ZnO thin film and their use. In section 3, materials and methods have been outlined, including how it was prepared and the way it was characterized in the study. Section 4 shows the results, which are the structural and optical properties of the ZnO films under different deposition cycles, followed by a discussion of these results. Lastly, Section 5 provides the conclusion of the paper where the main findings have been summarized, and suggestions have been presented on how to improve the performance of ZnO thin films in practical uses.

## LITERATURE SURVEY

Within the last few years, a considerable amount of attention has been paid to ZnO thin films due to the implementation of multiple application functions and the variety of technological applications. Many studies have been done to investigate different methods of deposition, including chemical bath deposition, sputtering, spray pyrolysis, and, most specifically, Successive Ionic Layer Adsorption and Reaction (SILAR), to enhance the quality of films without causing a significant rise in expenses. It has been demonstrated that ZnO thin films have high electron mobility, transparency in the visible region, as well as great photoluminescence and good applications in the field of optoelectronics, ultraviolet photodetectors, and transparent conductive oxides [8]. The low temperature of processing and simplicity of procedure of the SILAR method have made it a favorite option in the creation of ZnO films on flexible and temperature-sensitive substrates.

Recent studies have aimed at optimizing the structural and optical characteristics of ZnO thin films using different parameters of precursor concentration, deposition cycles, pH, and annealing conditions [10]. These parameters have been proven to play a major role in crystal orientation, grain size, uniformity of film, and defect density. As an example, the deposition time or the number of cycles has been observed to enhance the desired crystallinity and selective growth of specific crystal planes, which, in turn, influences the optical absorption edge and the values of the band gap. Comparisons of ZnO films drawn by various techniques all indicate that controlled deposition results in better film uniformity and optoelectronic qualities that can be used in photovoltaic and sensing devices.

Research has also explored the relationship that exists between morphological characteristics and functional performance. Better surface morphology with low roughness is linked to better charge transportation and less scattering loss, which is essential for device efficiency. It is reported that an optimum deposition utilizing cycle can lead to films with fewer voids, enhanced interconnections of the grains, and the reduction of surface defects. These enhancements can usually be converted into an increased optical transmittance, reduced resistivity, and increased defect-related emission, allowing improved operation in other applications like dye-sensitized solar cells, gas sensors, and light-emitting diodes.

Based on the literature reviewed, it is evident that the synthetic parameters, especially the deposition cycle count, are critical in dictating the structural, optical, and electronic characteristics of ZnO thin films. Nonetheless, as numerous works describe the overall tendencies, there is still a necessity to conduct systematic research according to which the impact of certain changes in the number of cycles on the main features of the film is measured. This gap supports the rationale of the current work, which seeks to offer an in-depth discussion of the impact of different deposition cycles on the nature of ZnO thin films produced using the SILAR technique regarding their structural and optical characteristics.

## MATERIALS AND METHODS

The methodology describes the procedure of deposition of ZnO thin films by the Successive Ionic Layer Adsorption and Reaction (SILAR) process. This is done by taking substrates and putting them in a

cationic and anionic precursor solution and rinsing with deionized water to encourage film formation. The procedure is continued through numerous cycles to obtain the required film aspect and characteristics.

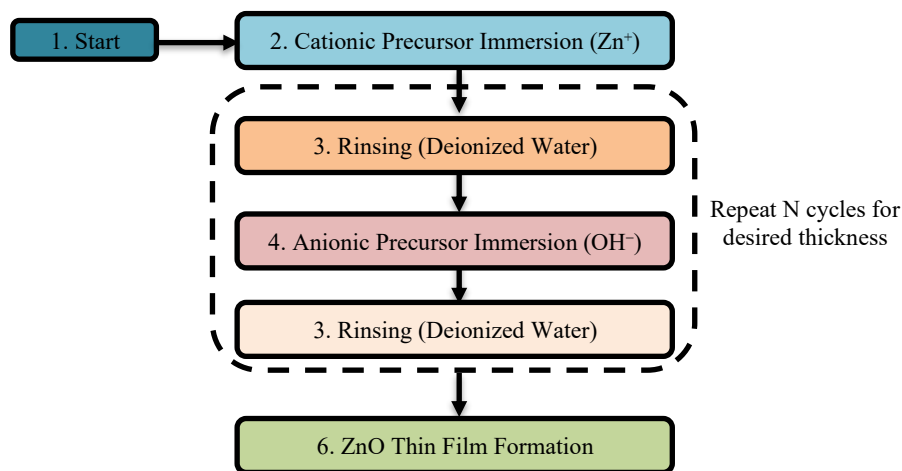


Figure 1. SILAR process for ZnO thin film deposition

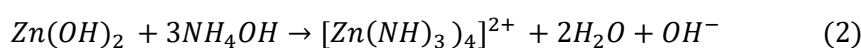
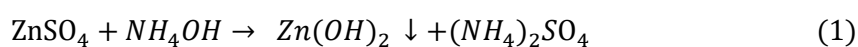
In figure 1 describes the process of depositing the ZnO thin films in the form of a flowchart, which includes the Successive Ionic Layer Adsorption and Reaction (SILAR) process. It involves five major steps 1) Start, 2) Cationic Precursor Immersion (Zn<sup>2+</sup>), 3) Rinsing with Deionized Water, 4) Anionic Precursor Immersion (OH<sup>-</sup>), 5) ZnO Thin Film Formation. The repetition of the process is done to a certain number of cycles in order to attain the required film thickness. This technique allows the deposition of ZnO thin films on substrates in a way that allows a controlled deposition and possesses better structural and optical characteristics.

### Technique Used for the Formation of Thin Films

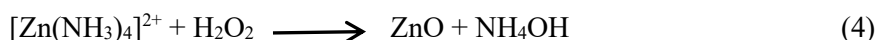
In this study, a ZnSO<sub>4</sub> solution of 0.2 M was mixed with an aqueous solution of ammonia (30% NH<sub>4</sub>OH) until the pH reached approximately 12. This mixture served as the cationic source, while H<sub>2</sub>O<sub>2</sub> of 2% concentration worked as the anionic source, with the reaction implemented at room temperature (300 K). Each glass substrate was washed with distilled water and then desiccated by passing hot air over its surface. Afterward, the glass substrate was vertically immersed in a solution of alkaline zinc sulfate to promote the adsorption of the zinc complex onto its surface. An adsorption reaction of the zinc complex and H<sub>2</sub>O<sub>2</sub> occurred after the substrate was immersed in H<sub>2</sub>OH, leading to the formation of ZnO thin films. The adsorption and reaction times were set to 20 and 30 seconds, respectively. Four deposition cycles were implemented, each repeated 5, 15, 20, and 25 times to increase the thicknesses of ZnO thin films. After completing the cycles, the substrates are removed from the solution and subsequently rinsed with a stream of dry air.

### Chemical Nucleation

To investigate the deposited ZnO thin films formed by the SILAR method on a substrate of glass. Two containers were prepared: the first one contained a ZnSO<sub>4</sub> solution with the tetra ammonium zinc (II) complex [Zn(NH<sub>3</sub>)<sub>4</sub>]<sup>2+</sup>, which was prepared by adding an excess of ammonia as stated by the reaction that is shown in equations (1) and (2). The second one was filled with (H<sub>2</sub>O<sub>2</sub>) solution that dissolved in water, as described by the reaction that is shown in equation (3) [9]:



Upon immersion of the substrate in the first container, the adsorption process immediately begins on its surface [9]. As the H<sub>2</sub>O<sub>2</sub> solution is considered an oxidizing agent, the zinc that is precipitated as a coating on the glass's surface is oxidized immediately after immersing the coated substrates in the H<sub>2</sub>O<sub>2</sub> solution. The reaction is represented by the following equation (4):



### Examination Method

The samples were subjected to X-ray analysis (1.54Å<sup>0</sup>) to identify the structural properties, such as lattice parameters, grain size, dislocation densities, and average crystallite size of ZnO thin films. Additionally, spectrophotometer of UV–VIS–NIR used to inspect the optical properties. It used a wavelength range (200-900nm) due to the limitations of lattice dimensions.

## RESULT AND DISCUSSION

### Structural Properties

In figure 2 shows the pattern of X-ray diffraction used to determine the structural properties of thin films of ZnO and identify the forming phases. The results confirmed that the prepared thin films demonstrated a polycrystalline microstructure with a hexagonal wurtzite structure. X-ray line profile revealed that the preferred orientation of crystals is along the (100) plane, as is evident in a diffraction peak at 2θ = 31.67°. Additionally, the crystallites have predominantly oriented along the c-axis, which is orthogonal to the surface of the substrate that contains the deposited ZnO. Phase identification and comparison between experimental findings and standard interplanar spacings (d-values) were performed with the aid of the JCPDS database (card no. 36–1451); the results are summarized in table 1.

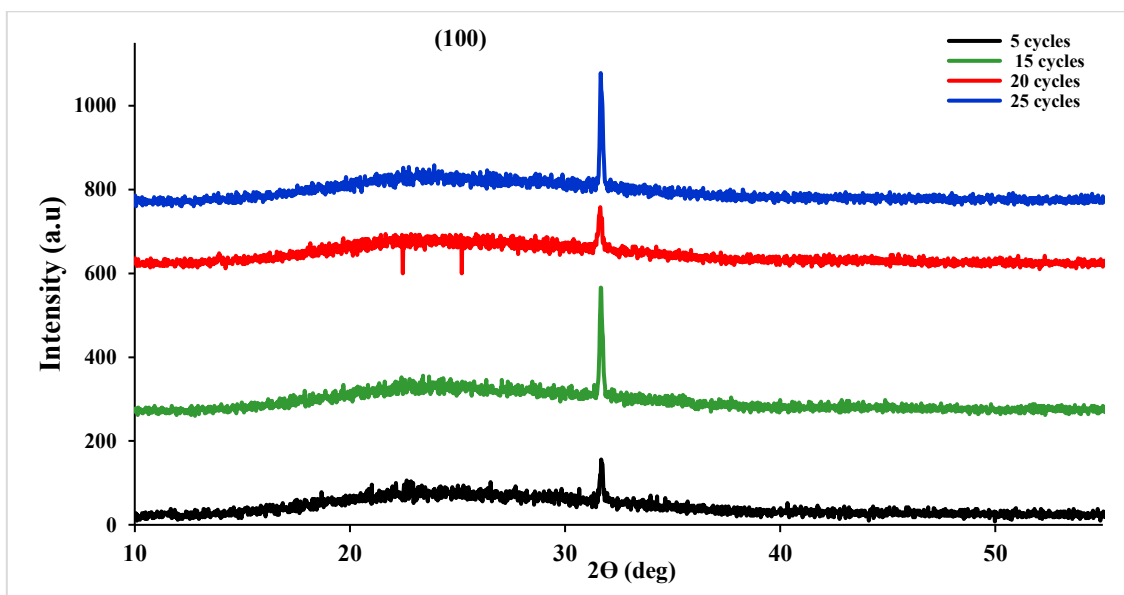


Figure 2. XRD line profile for the ZnO thin films

Experimental data showed that the lattice parameters of the crystal (a and c) are altered. Also, the d-value, which represents the inter-planar space for Miller indices h, k, and l, began with a relatively small value (2.8190 Å<sup>0</sup>) and continued to increase to reach 2.824560 Å<sup>0</sup> in the case of the 15-cycle sample. Then, this behavior was changed by dropping the value to 2.82012 Å<sup>0</sup> as the number of cycles was increased to 25, as evaluated via the equation (5) [11].

$$\frac{1}{d_{hkl}^2} = \frac{4(h^2 + k^2 + l^2)}{2a^2} + \frac{l^2}{c^2} \quad (5)$$

Furthermore, the value of (a) shows an increase in its values as the number of cycles increases from 5 cycles to 20 cycles, then it drops for the sample of 25 cycles. However, this behavior differs slightly for the c-value, as its value increases with the cycle number, as shown in table 1.

Table 1. Stated the determined parameter values for the crystal lattice and the size of grains

No. of Cycle	d(Å) Measured	d(Å) Standard	Miller Indices (hkl)	a (Å)	c(Å)	Average Grain Size (nm)
5 cycles	2.8191	2.8142	100	3.2552	5.05310	50.728
15 cycles	2.820681		100	3.2563	5.18620	55.95
20 cycles	2.824561		100	3.2616	5.2012	39.78
25 cycles	2.820121		100	3.2565	5.2648	63.52

The average grain size of the ZnO thin film was calculated using Scherrer's formula, which exhibits an inverse relation between the grain size and the full width at half maximum (FWHM), as stated in equation (6) [12].

$$D = \frac{0.9*\lambda}{B\cos \theta} \tag{6}$$

$\lambda$  represents the wavelength of the x-ray that was used, B is the full width at half maximum and  $\theta$  represents the angle of Bragg.

A prominent diffraction peak at  $2\theta = 31.67^\circ$  indicates that highly crystalline structures are formed in the samples under investigation. This diffraction peak corresponds to a larger grain size (63.51 nm) that formed in the sample after 25 cycles, compared with the rest of the samples. Additionally, dislocation density ( $\delta$ ), which represents the amount of defects within the formed structure of the thin films, drops as the grain size increases, as stated in table 2. Specifically, the value of dislocation density in the case of the 5-cycle sample was  $3.88591 \times 10^{14}$  lines/cm<sup>2</sup>, while this value decreased to around  $2.479 \times 10^{14}$  lines/cm<sup>2</sup> in the case of the sample of 25 cycles. This suggests crystallinity and film quality improved in the latter case of the thin film. Moreover, the density of crystallites per unit surface area (N) was calculated using equation (7) as follows [13][14]:

$$N = \frac{t}{D^3} \tag{7}$$

The symbol t denotes the thickness of the formed thin film, which was determined using a gravimetric method and found to be approximately 4 nm. In table 2 states the structural characteristics of the samples, including dislocation density and strain.

Table 2. Presents the structural properties, including the dislocation value and Strain related to the formed thin film

No. of Cycle	Dislocation Value (line/cm <sup>2</sup> )	Density of Crystallites Per Unit Surface Area (N) (m <sup>-2</sup> )	Strain S%
5 cycles	38.86*10 <sup>13</sup>	51.077E+17	2.9481
15 cycles	31.94*10 <sup>13</sup>	37.880E+17	0.3922
20 cycles	63.177*10 <sup>13</sup>	10.765E+18	0.1023
25 cycles	24.790*10 <sup>13</sup>	26.105E+17	1.1192

$C_{XRD}$  consistently measures strain (S) and identifies the deviation from the ASTM standard value; this parameter is calculated by the following equation (8).

$$S = \frac{|C_{ASTM}-C_{XRD}|}{C_{ASTM}} * 100\% \tag{8}$$

$C_{ASTM}$  refers to c-lattice constant, which agrees with the values of  $A_{STM}$  card, while  $C_{XRD}$  represents the c-lattice constant that is determined using the XRD technique. The conditions of the deposition process used in this work have a significant influence on the strain value, whether the formed strain is positive (tensile) or negative (compressive), by varying the lattice constant value from its value compared with the  $C_{ASTM}$  standard. However, the experimental results exhibited that the behaviour of the formed strain is inversely proportional to the increasing number of cycles, as the strain decreased from 2.948 to 1.119 when the cycles changed from 5 to 25. This relation between strain and cycle number is associated with the increasing grain size; this result is consistent with and supported by the studies demonstrated in [7][8]. In other words, the strain value directly proportional to the variance of  $C_{XRD}$  as stated in the  $A_{STM}$  standard.

### Optical Properties

The investigation of optical properties is achieved by using UV light of wavelengths extended over 250 to 1050 nm, as shown in figure 3. First, the transmittance values for the thin films that are formed by four different cycles are measured; their value rapidly increased when the applied wavelength reached around 325 nm, as shown in figure 3a. The figure also shows that the sample with fewer cycles (5 cycles) exhibits a lower transmittance value compared to the other samples (15, 20, and 25 cycles). This behavior is attributed to the increased grain boundary density due to smaller grain size; hence, the scattering of light within the thin film becomes more pronounced in the case of the 5-cycle sample, leading to reduced transmittance [11][13][20].

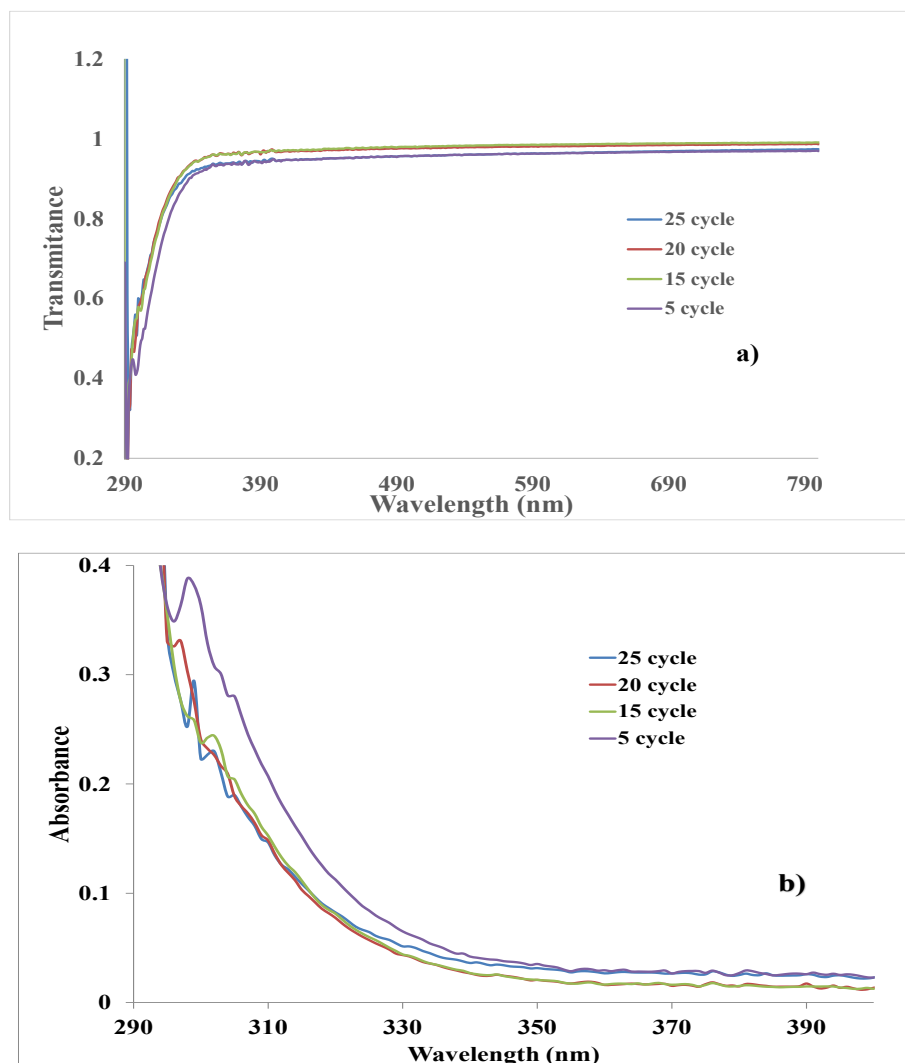


Figure 3. (a) Shows the transmittance, and (b) shows the absorption for the produced thin films by conducting them into UV-visible spectroscopy

In figure 3b shows the relationship of absorption of each sample with wavelength applied by the UV equipment; this profile shows that the first sample (5 cycles) is characterized by a higher absorbance compared with the rest of the samples. It has a peak value at (0.39) near the applied UV wavelength light, and that is preferred for solar cell applications. As the number of cycles increases from five to 25 cycles, the results demonstrate a reduction in the absorbance value as it drops from 0.39 to 0.27 at the same wavelength (300nm). Nevertheless, all samples exhibited a rapid drop in the absorbance value with increasing wavelength at 310 nm, whereas the sample of 5 cycles consistently showed the highest absorbance compared with the other samples. When the energy of the conducted UV light on the thin film of the sample corresponds to the energy of the band gap of the crystal that formed the thin film, a significant absorption occurs, as illustrated in the line profile at wavelengths lower than 310 nm shown in figure 3b. In contrast, when the wave's energy of the incident UV light on the sample does not correspond to the band gap of the crystal that formed the thin film, this wave will not be absorbed by the crystals of the thin film, thus resulting in low absorption as shown on the line profile at wavelengths higher than 310 nm that are shown in figure 3b.

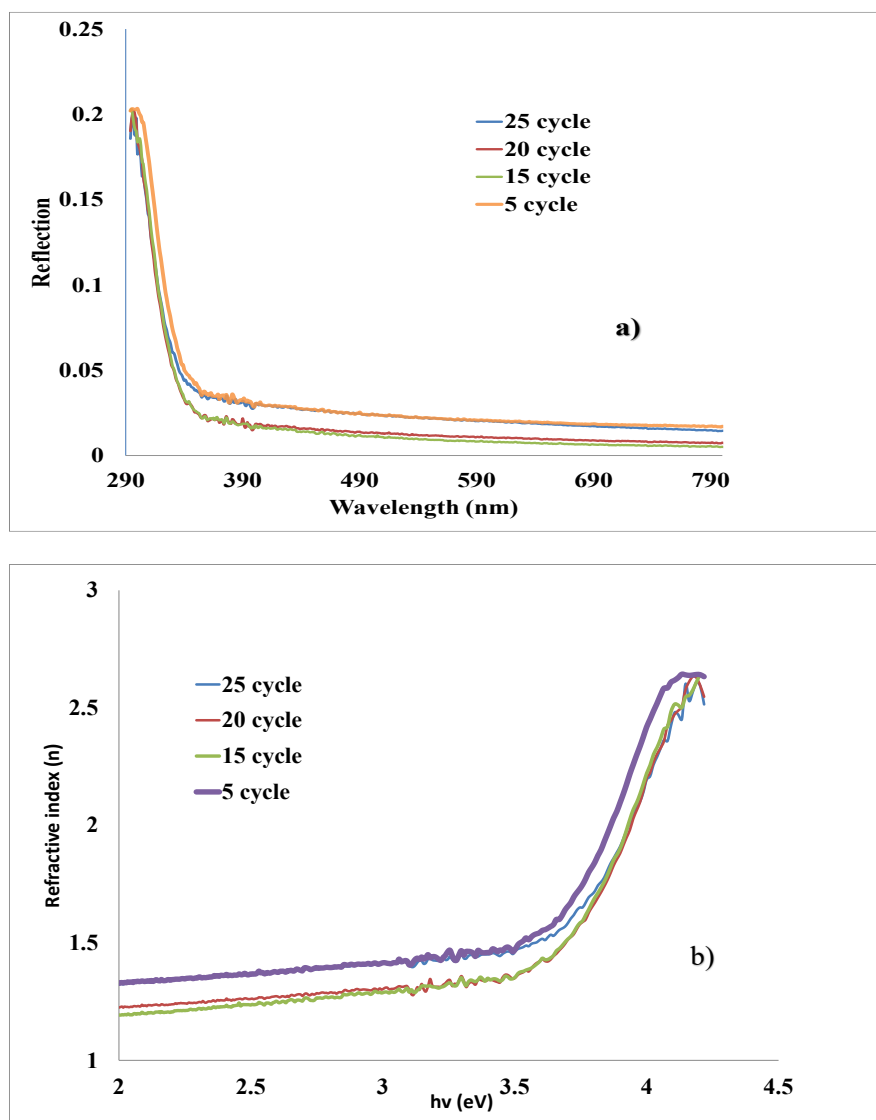


Figure 4 (a). Shows the relation of the reflection index with the wavelength, while figure 4(b) depicts the change in refractive index as a function of the energy gap

In figure 4 shows the reflection and refractive index values over a wide range of applied wavelength that changes from the UV to the IR region. Figure 4a shows that the reflection values drop rapidly as the wavelength changes in the UV region (at 354 nm). Figure 4a shows that the reflection values dropped rapidly over the changing wavelength in the UV region, while the line profile of samples 15 and 20

cycles showed they retained their higher values compared to samples 5 and 25 cycles along all wavelengths used in this investigation.

In figure 4b. shows the refractive index values, which revealed that the value for the two samples of 5 and 25 cycles is higher compared with the two other groups of samples (15 and 20 cycles), it was 1.33 and 1.2 at the energy gap of 2 eV, respectively. As well as the refractive index (n) increased rapidly from 1.56 and 1.43 to reach around 2.6 as the band gap energy increases from 3.62 eV to around 4.2 eV for the (5 and 25 cycles) and (15 and 20 cycles) groups, respectively.

In figure 5 demonstrates the type of band gap value for all the samples under consideration; this type can be calculated by Tauc formula [14, 15].

$$\alpha h\nu = C(h\nu - E_g)^m \tag{9}$$

In equation (9), where  $E_g$  represents the energy gap between the lowermost of the conduction band and the topmost of the valence band, and  $h\nu$  is the energy of the incident photon.

The calculations show the value of band gap energy for the (5-cycle) sample is (3.67 eV), and this value increased as the number of cycles increased to 15 and 20 cycles to become (3.69 eV and 3.81 eV), respectively. However, its value reduced for the last sample (25 cycles) to become (3.8 eV). As a result, it can be seen clearly in the graph of  $(\alpha h\nu)^2$  versus band gap energy that the band gap for this structure is of a direct type.

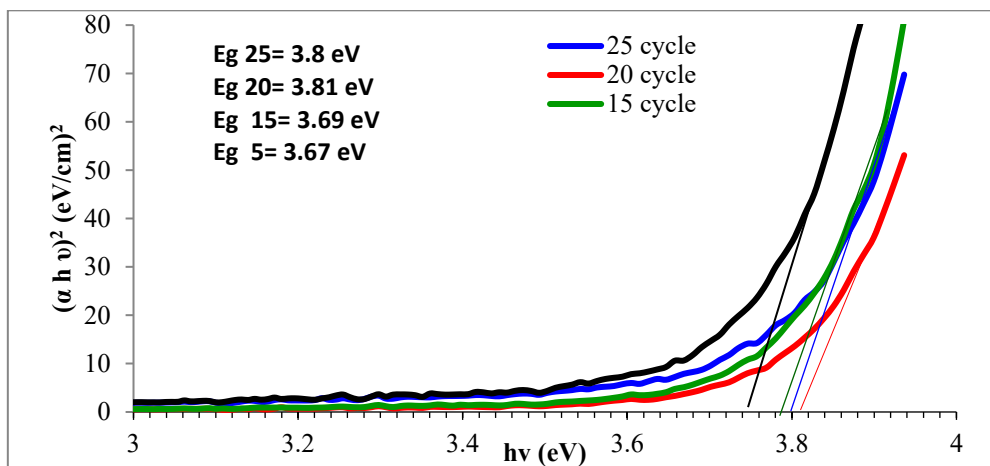


Figure 5. Shows the type of band gap energy with its values

The absorption coefficient ( $\alpha$ ) was evaluated from the absorbance spectra utilizing formula (10) [15].

$$\alpha = \frac{2.303 A}{t} \tag{10}$$

In equation (10), where A and t are the absorbance and thickness of the films, respectively.

The experimental results of figure 4 showed that the energy gap coincides with the results of figure 6. It has been proven that these films have respectable absorption characteristics in the UV spectra. This demonstrated that the films of ZnO can be applied to the solar cell as transparent windows.

$$K = \frac{\alpha \lambda}{4\pi} \tag{11}$$

In equation (11), where (K) represents the extinction coefficient factor that shows the fraction of light, which is lost due to the absorption and scattering of incident light per unit distance of the medium [16][17][18].

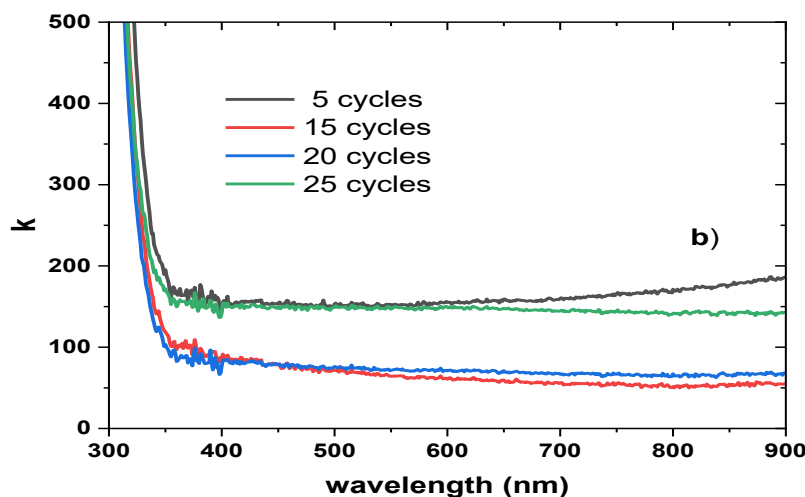


Figure 6. (a) Shows the absorption coefficient with energy gap, (b) the extinction coefficient factor versus wavelength

The figure 6a. shows an increment in extinction coefficient values gradually and shifts toward higher energies as cycles increase, while the absorption coefficient shifted to a lower energy gap as shown in figure 6b. The results show that two samples of 5 and 25 cycles absorb light more efficiently, so they appear opaque and shiny compared with the two samples (15 and 20 cycles, respectively) at the wavelength higher than 375 nm, while all samples have similar absorption at wavelengths lower than 375 nm. This illustrates how the reflectivity of samples of 5 and 25 cycles also increases while their transmittance is lower compared to samples (15 and 20 cycles, respectively).

## CONCLUSION

ZnO thin films were also obtained through the SILAR technique in this paper, with deposition cycles of 5, 15, 20, and 25 cycles, to evaluate the structural and optical characteristics of ZnO films. The analysis using X-ray diffraction (XRD) showed that the material was polycrystalline and hexagonal in nature with preferential orientation on the (100) plane. The size of the grain was proportional to the deposition cycles, and the density of dislocations was reduced, which means the quality of the film and crystallinity were improved. The optical band gap was between 3.67 eV and 3.81 eV, with the largest being recorded in the case of the 20-cycle sample, which shows the impact of deposition cycles on the optical properties of the film. The absorbance was low at a high cycle number, which was associated with increased scattering and a greater level of control over the grain boundaries. These results imply that the SILAR technique is a low-cost technology to produce ZnO thin films with customized properties to be used in different optoelectronics. Future studies can be done on how to tailor the other parameters of deposition which include the precursor concentration and the annealing temperature in order to further improve the characteristics of ZnO thin films. Also, the prospect of the incorporation of these movies into practical products, including solar cells, sensors, transparent conductive surfaces, etc., may shed more light into the real-world applications of these movies. More research might also be done to determine the stability and performance of the ZnO films on a long-term basis in the real-life scenarios in order to guarantee their functionality in the business world.

## REFERENCES

- [1] Hongsingthong A, Yunaz IA, Miyajima S, Konagai M. Preparation of ZnO thin films using MOCVD technique with D2O/H2O gas mixture for use as TCO in silicon-based thin film solar cells. *Solar Energy Materials and Solar Cells*. 2011 Jan 1;95(1):171-4. <https://doi.org/10.1016/j.solmat.2010.04.025>
- [2] Naeem S, Husain D, Ahmad S, Faisal S, Ansari Y, Patil AV. Investigating the electrical and thermal properties of Cu and Al-doped ZnO thick films using the screen-printing technique for thermal resistance applications. *Journal of the Indian Chemical Society*. 2024 Oct 1;101(10):101292.

- <https://doi.org/10.1016/j.jics.2024.101292>
- [3] Wagh RV, Yewale CR, Deshmane VV, Tupe UJ, Mandawade SS, Patil AV. Synthesis and Characterization of Tin Sulfide (SnS<sub>2</sub>) Thin Films and Its Application for Hazardous Gas Detection. *Total Chemistry*. 2025 Sep 10;100012. <https://doi.org/10.1016/j.totche.2025.100012>
- [4] Barkat H, Guettaf Temam E, Ben Temam H, Mokrani N, Rahmane S, Althamthami M. Thickness-dependent photocatalytic performance and wettability of barium-doped ZnO thin films synthesized via SILAR technique. *Transition Metal Chemistry*. 2025 Aug;50(4):431-50. <https://doi.org/10.1007/s11243-025-00631-z>
- [5] Desai MA, Sartale SD. Facile soft solution route to engineer hierarchical morphologies of ZnO nanostructures. *Crystal Growth & Design*. 2015 Oct 7;15(10):4813-20. <https://doi.org/10.1021/acs.cgd.5b00561>
- [6] Ali RS, Sharba KS, Jabbar AM, Chiad SS, Abass KH, Habubi NF. Characterization of ZnO thin film/p-Si fabricated by vacuum evaporation method for solar cell applications. *NeuroQuantology*. 2020 Jan 1;18(1):26-31. <https://doi.org/10.14704/nq.2020.18.1.NQ20103>
- [7] Sreedev P, Rakshesh V, Roshima NS, Shankar B. Preparation of Zinc Oxide Thin films by SILAR method and its Optical analysis. In *Journal of Physics: Conference Series* 2019 Mar 1 (Vol. 1172, No. 1, p. 012024). IOP Publishing. <https://doi.org/10.1088/1742-6596/1172/1/012024>
- [8] Kumar N, Dubey A, Bahrami B, Venkatesan S, Qiao Q, Kumar M. Origin of high carrier mobility and low residual stress in RF superimposed DC sputtered Al doped ZnO thin film for next generation flexible devices. *Applied Surface Science*. 2018 Apr 1;436:477-85. <https://doi.org/10.1016/j.apsusc.2017.11.274>
- [9] Jambure SB, Patil SJ, Deshpande AR, Lokhande CD. A comparative study of physico-chemical properties of CBD and SILAR grown ZnO thin films. *Materials research bulletin*. 2014 Jan 1;49:420-5. <https://doi.org/10.1016/j.materresbull.2013.09.007>
- [10] Ismail AS, Mahmud QH. Study the Influence of Tin Oxide SnO<sub>2</sub> Doping on the Optical and Structural Properties of Titanium Oxide TiO<sub>2</sub>. *International Academic Journal of Innovative Research*. 2024;11(1):61-5. <https://doi.org/10.9756/IAJIR/V11I1/IAJIR1107>
- [11] Alkhayatt AH, Hussian SK. Fluorine highly doped nanocrystalline SnO<sub>2</sub> thin films prepared by SPD technique. *Materials Letters*. 2015 Sep 15;155:109-13. <https://doi.org/10.1016/j.matlet.2015.04.130>
- [12] Thahab SM, Alkhayat AH, Saleh SM. The optical properties of Cd<sub>x</sub>Zn<sub>1-x</sub>S thin films on glass substrate prepared by spray pyrolysis method. *Optik*. 2014 Sep 1;125(18):5112-5. <https://doi.org/10.1016/j.ijleo.2014.05.014>
- [13] Bourebia A, Bouaine A, Guendouz H. Appearance of amorphous phase in crystalline In-Y codoped ZnO thin films. *Bulletin of Materials Science*. 2024 Apr 29;47(2):89. <https://doi.org/10.1007/s12034-024-03146-y>
- [14] Jubu PR, Obaseki OS, Ajayi DI, Danladi E, Chahrour KM, Muhammad A, Landi Jr S, Igbawua T, Chahul HF, Yam FK. Considerations about the determination of optical bandgap from diffuse reflectance spectroscopy using the Tauc plot. *Journal of Optics*. 2024 Nov;53(5):5054-64. <https://doi.org/10.1007/s12596-024-01741-0>
- [15] Haneen Abass K, Haidar Obaid N. 0.006 wt.% Ag-Doped Sb<sub>2</sub>O<sub>3</sub> nanofilms with various thickness: morphological and optical properties. In *Journal of Physics: Conference Series* 2019 Sep 1 (Vol. 1294, No. 2, p. 022005). IOP Publishing. <https://doi.org/10.1088/1742-6596/1294/2/022005>
- [16] Abd El-Ghany WA. Review on the optical and electrical properties of chalcogenide thin films: challenges and applications. *Physical Chemistry Chemical Physics*. 2025;27(9):4567-86. <https://doi.org/10.1039/D4CP04473H>
- [17] Raut P, Panda DK, Goyal AK. A Comprehensive Review on Next-Generation Modelling and Optimization for Semiconductor Devices. *IEEE Access*. 2025 Jul 10;13: 123724 - 123742. <https://doi.org/10.1109/ACCESS.2025.3587721>
- [18] Mohamed AM, Hwail HM, Hassan AM, Almayahi BA. Prepared Panel and Film from Nano pigment it used to Improve the Efficiency Conversion of Solar Cells. *Natural and Engineering Sciences*. 2025 Jan 9;10(2):231-8. <https://doi.org/10.28978/nesciences.1733120>
- [19] Ismail A, Abdullah MJ. The structural and optical properties of ZnO thin films prepared at different RF sputtering power. *Journal of King Saud University-Science*. 2013 Jul 1;25(3):209-15. <https://doi.org/10.1016/j.jksus.2012.12.004>
- [20] Yergaliuly G, Soltabayev B, Kalybekyzy S, Bakenov Z, Mentbayeva A. Effect of thickness and reaction media on properties of ZnO thin films by SILAR. *Scientific reports*. 2022 Jan 17;12(1):851. <https://doi.org/10.1038/s41598-022-04782-2>